Case Study of Petrophysical Evaluation Utilizing Well Logs Data with Optimization of Reservoir Cut-off Parameters

Walid Mohamed Mahmud[1*] and Ziad Bennour[2]

[1]*Department of Petroleum Engineering, Faculty of Engineering, University of Tripoli, Tripoli, Libya*

[2]*Petroleum Engineering Department, Curtin University Malaysia, CDT250, Miri 98000, Sarawak, Malaysia*

Abstract: Petrophysical evaluation of well log data is essential for the exploration and evaluation of hydrocarbon-bearing formations. Moreover, there are no standard criteria to implement cut-offs on petrophysical properties as a direction for economic decisions. In the present work, a petrophysical evaluation of well logging data from four wells in a mature oil field is performed to identify formation quality as a potential for hosting mature hydrocarbons reservoirs. Full consideration of cut-off values was taken into account. The cut-offs were estimated from well-recognized petrophysical relationships for permeability as a function of porosity, water saturation, and shale content. Results verification and calibration were also made based on laboratory measurements of petrophysical properties obtained from available core plugs in order to minimize uncertainty. Lithology analysis and characteristics revealed that the target formation is mainly sand and shale sequences. Results from well logs were in agreement with results obtained from core data. Formation effective porosity varies from 16 to 26% in all wells. A wide range of variations is observed in water saturation ranging from 28 to 57% and permeability ranging from 20 to 3300 mD. This is in good agreement with other measurements and well log analysis that show the mature formation remains to be a good hydrocarbon reservoir with significant potential.

Keywords: Well log analysis, cut-offs in integrated reservoir studies, petrophysical properties, experimental measurements, mature fields, shaly sands.

1. INTRODUCTION

1.1. Well Logging and Reservoir Characterization

Evaluation of petrophysical properties through well-logging data is a necessity for the recognition and assessment of hydrocarbons (HC) presence in a reservoir. Quality of well logging data also plays a significant role in determining HC production potential as well logging data are regularly utilized for seismic velocity calibration, wavelet estimation, low-frequency model building, and time-to-depth conversion that yield a high-quality seismic reservoir description [1]. Several studies [2-5] have concluded that relationships between various petrophysical parameters, reservoir characterization, and production rate analysis minimize reservoir evaluation uncertainty. Evaluation of subsurface formation petrophysical properties using well logs, well test, and core data can be a source of information on many reservoir properties such as lithology, permeability, porosity, clay volume, grain size, fluid saturation, and net pay thickness. This information is important for reservoir characterization [6-10]. However, the prediction of these properties is complex, as the measurement locations are settled at widely spaced intervals. The traditional technique used to identify lithofacies is through direct observation of subsurface cores [11-13]. Direct observation from core data to determine lithology is precise. However, the analysis route is lengthy, costly, and not always consistent.

Effective reservoir management requires an accurate reservoir geological description and properly identifies reservoir hydrocarbon reserve. Geological attributes, distribution and reservoir formation pore space can be attained from information such as well test data, production data, well logs and cores data in order to accurately describe a reservoir. In addition to reservoir properties, reservoir cleanliness or shaliness is an additional parameter that is considered for reservoir characterization as it affects the estimation of other reservoir petrophysical properties [14]. Therefore, hydrocarbon reserve evaluation, determination of formation thickness and depth, the distinction between formation fluids and correlation of hydrocarbon accumulation zones maybe estimated by well logs [15]. Reservoir engineers, geoscientists, and petrophysicists utilize practical cut-off and net-to-gross parameters to delineate a reservoir's hydrocarbons economic value. These parameters are coupled with mathematical modeling to set completion intervals and predict production rates that are critical for reservoir evaluation. The net-to-gross or pay fraction is the formation thickness containing hydrocarbons in a given interval. However, the cut-off is a particular criterion that has to be met in order to recognize a hydrocarbon-containing zone as a pay zone. Therefore, the cut-off is the limiting value of any particular property (i.e., oil saturation, porosity and permeability) used to exclude rocks that do not effectively participate in reservoir economic evaluation [16].

Lithology logs of a neutron, gamma ray, deep and shallow resistivity and density were utilized in the present study to evaluate hydrocarbon potentials.

*Address correspondence to this author at the Department of Petroleum Engineering, Faculty of Engineering, University of Tripoli, Tripoli, Libya;
E-mail: W.Mahmud@uot.edu.ly

E-ISSN: 2409-787X/20

Available formation petrophysical properties estimated by well logs were used to explore potential relationships between petrophysical properties and other different reservoir parameters. Thus, the aim of the present study was to evaluate the remaining hydrocarbon potential in a mature field using lithology identification and petrophysical analysis.

1.2. The Study Site

Hydrocarbon exploration and production in Sirte Basin started in the late 1950s. Therefore, discoveries were assumed as matured oil fields [17]. Sirte basin was considered one of the most productive oil-producing fields in the world and their viable production continues until now. Sirte basin is one of four well-known sedimentary basins in Libya located in the country's north-central part. The basin spans over an area of around 600,000 km² and is considered the youngest and richest hydrocarbons' basins in Libya. The basin developed in the late Paleozoic through much of the early Cretaceous with continuous uplift that formed the Sirte arch. From the start of the Late Cretaceous, extensional tectonics caused a partial collapse of the arch that led to the development of horsts and grabens system, as shown in Figure **1** [18-20]. Giant oil fields such as Amal, Sarir, Raguba, and Zelten were found between 1956 and 1961 [21,22]. Compared to the North Sea, which is heavily explored three times more than the Sirte basin, the Sirte basin still has a real significant future explorations potential [23,24].

The study site, A-field, is located on the Beda Platform with a surface area of approximately 4,708 km^2 and around 135 km to the south of the Mediterranean Sea.

2. METHODS

The A-field was initially producing approximately 400M bbl/d of crude oil, which then accounted for about one-third of Libya's oil production. During the drilling and investigation activities, different open hole logs were run, and core plugs were extracted to evaluate and determine the formations' petrophysical properties. Four wells were selected from the A-field to represent the target formation. Well logging tools were initially corrected for the borehole environmental effects and then calibrated. The log suite was one of the essential tools used to estimate natural radioactivity in the formations in order to identify different lithologies of shales and clays from reservoir rocks and to determine fluid saturation profiles. The density log measured formation bulk density that was a key tool for porosity measurement. Neutron porosity tool measured the hydrogen index that reflected fluid type in the void spaces. The sonic log was used to determine porosity by charting the speed of a compressional sound wave as it traveled through the formation. Log

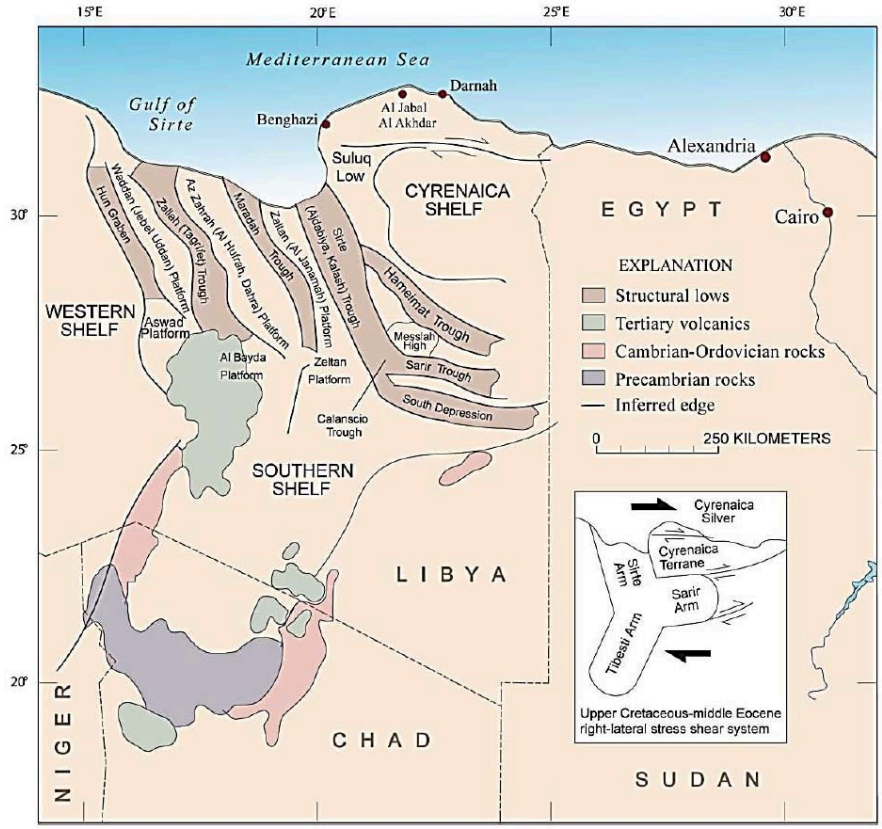

Figure 1: Structural elements of Sirte basin. Barbs show direction of relative movement on faults [17].

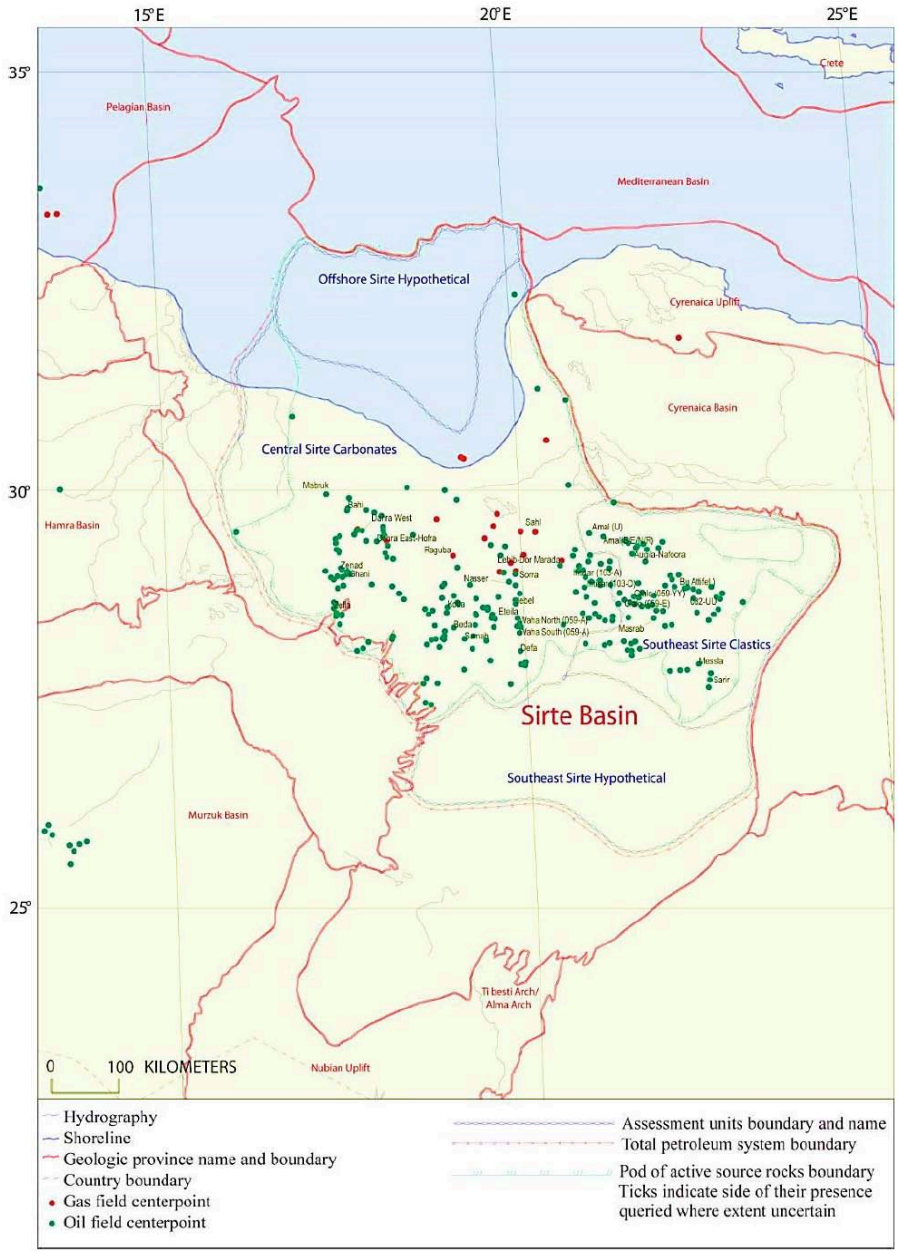

Figure 2: Sirte-Zelten boundaries of petroleum systems, pods of active source rock, and oil and gas field center points, modified: Thomas [17].

measurements were taken for every 0.5ft of depth for the subjected wells. The following sections describe the equations and methods used to estimate the petrophysical property parameters.

2.1. Shale Volume Determination

$$I_{GR} = \frac{GR(Log) - GR(min)}{GR(Log) - GR(min)} \quad (1)$$

Where:

I_{GR}: Describes a linear response to shale line or clay content (API)

GR (log): gamma-ray reading at the log interval

GR (min): minimum gamma-ray reading

GR (max): maximum gamma-ray reading.

Thus, the shale volume (V_{sh}) equals the gamma-ray index (I_{GR}).

2.2. Porosity

Formation bulk density (ρ_b) is a function of matrix density, matrix porosity, and fluid density in the pores, i.e., brine, mud, or hydrocarbons. Table **1** provides the matrix densities for sandstone, limestone, dolomite, and anhydrite used to calculate density log porosity:

Table 1: Matrix Densities of Common Lithologies [27]

Matrix	ρ (gm/cc)
Sand Stone	2.648
Limestone	2.71
Dolomite	2.876
Anhydrite	2.977

The formula for calculating porosity from the density log is:

$$\emptyset = \frac{\rho_m - \rho_b}{\rho_m - \rho_f} \quad (2)$$

Where:

ρ_b: formation bulk density, gm/cc (log).

ρ_f: fresh fluid density that equals 1gm/cc.

ρ_m: matrix density established at 2.65 gm/cc for sandstone formation.

As the volume of shale (V_{sh}) is calculated, it is used to correct the shale effect on the porosity log. The formula of the density log as follows [25,27]:

$$\emptyset_{\mathrm{den}} = \frac{\rho_m - \rho_b}{\rho_m - \rho_f} - \mathrm{V_{sh}}\left(\frac{\rho_m - \rho_{sh}}{\rho_m - \rho_f}\right) \quad (3)$$

Where:

V_{sh}: volume of shale

$\emptyset_{den}$: porosity corrected for shale.

The Combination Neutron-Density log is a combination porosity log. Besides its use as a porosity device, the porosity from the Neutron-Density log can be calculated mathematically. The alternate method of determining Neutron-Density log porosity [25] is to use the root mean square formula:

$$\emptyset_{\mathrm{N-D}} = \sqrt{\frac{\emptyset_N{}^2 + \emptyset_D{}^2}{2}} \quad (4)$$

Where:

$\emptyset_{\mathrm{N-D}}$: neutron-density log porosity.

$\emptyset_N$: neutron porosity (limestone units).

$\emptyset_D$: density log porosity (limestone units).

After the volume of shale (V_{sh}) is determined, it can then be used to correct the porosity log for the shale effect. The formula of Combination Neutron-Density log [25,27]:

$$\emptyset_{\mathrm{N-D}} = \sqrt{\frac{\emptyset^2_{Ncorr} + \emptyset^2_{Dcorr}}{2}} \quad (5)$$

Where:

$\emptyset_{\mathrm{Ncorr}}$: neutron porosity corrected for shale.

$\emptyset_{\mathrm{Dcorr}}$: density log porosity corrected for shale.

Interval transit time (Δt) depends on lithology and porosity. Thus, the known formation matrix velocity [27] is used to obtain the sonic porosity from the following formula:

$$\emptyset = \frac{\Delta \mathrm{t_{log}} - \Delta \mathrm{t_m}}{\Delta \mathrm{t_f} - \Delta \mathrm{t_m}} \quad (6)$$

Where:

Δt_m: interval transit time of matrix. In this study, Δtm equals 55.5 μsec/ft.

Δt_{log}: interval transit time of formation, μsec/ft.

Δt_f: interval transit time of the fluid in wellbore, μsec/ft.

Once V_{sh} is calculated, it is used to correct the shale effect in porosity log [25]. Thus, the porosity sonic log formula becomes:

$$\emptyset = \left(\frac{\Delta \mathrm{t_{log}} - \Delta \mathrm{t_m}}{\Delta \mathrm{t_f} - \Delta \mathrm{t_m}} \times \frac{100}{\Delta \mathrm{t_{sh}}}\right) - \mathrm{V_{sh}}\left(\frac{\Delta \mathrm{t_{sh}} - \Delta \mathrm{t_m}}{\Delta \mathrm{t_f} - \Delta \mathrm{t_m}}\right) \quad (7)$$

2.3. Formation Water Resistivity from SP Curve and Salinity

SP curve method provides somewhat less accurate water resistivity in shaly, hydrocarbon-bearing, and low porosity zones [27]. Therefore, we use Crain's model as following:

$$R_w = \left(\frac{\frac{400{,}000}{FT}}{W_S}\right)^{0.88} \quad (8)$$

Where:

R_w : formation water resistivity, ohm.m

FT: formation temperature, ^{0}F

W_S: water salinity, ppm

Formation water saturation (S_W) was determined from R_W that was corrected for shale and porosity using the following two equations, and the average value was implemented [25]:

Simandoux [28]:

$$S_W = \left(\frac{0.4\,\mathrm{R_w}}{\emptyset^2}\right) \times \left[-\frac{\mathrm{V_{sh}}}{\mathrm{R_{sh}}} + \sqrt{\left(\frac{\mathrm{V_{sh}}}{\mathrm{R_{sh}}}\right)^2 + \frac{5\emptyset^2}{\mathrm{R_t \times R_w}}}\right] \quad (9)$$

Schlumberger [29]:

$$S_W = \frac{-\frac{\mathrm{V_{sh}}}{\mathrm{R_{sh}}} + \sqrt{\left(\frac{\mathrm{V_{sh}}}{\mathrm{R_{sh}}}\right)^2 + \frac{\emptyset^2}{0.2\,\mathrm{R_w} \times \mathrm{R_t}(1-\mathrm{V_{sh}})}}}{\frac{\emptyset^2}{0.4\,\mathrm{Rw}\,(1-\mathrm{V_{sh}})}} \quad (10)$$

Where:

S_W: uninvaded zone water saturation corrected for volume of shale.

R_W: formation water resistivity at formation temperature.

R_t: true formation resistivity.

R_{sh}: resistivity of adjacent shale.

2.4. Permeability Estimation

Permeability is an essential tool in reservoir modeling; however, permeability estimation often poses a significant challenge to reservoir characterization and simulation. Log-derived method was used to calculate permeability:

$$k = \sqrt{\frac{250\,\emptyset^2}{S_{wir}}} \quad (11)$$

Where:

K: permeability, md

S_{wir}: Irreducible water saturation established at 0.27 from core data analysis [25].

Formation containing shale is detected by gamma-ray that distinguishes shale by its high radioactivity. Sandstone and carbonate formations that are shale-free have radioactive material of low concentrations; therefore, gamma-ray readings are low. If shale content radioactivity was constant with the absence of other radioactive minerals dissimilated in the formation, gamma-ray reading could be expressed as a function of clay content. Since shale is considered more radioactive than sand or carbonate, a gamma-ray log is used to calculate shale volume in a reservoir. Shale volume is utilized for shaly sands analysis, and a gamma-ray index is required first to calculate shale volume from the gamma-ray log.

2.5. Net Pay Thickness

Rock thickness that participates in economically applicable production in today's costs, prices, and technology is defined as net pay. Therefore, as costs, prices and technology continuously change at a rapid pace, the definition of net pay continuously changes. For instance, new technology enables the depletion of tight reservoirs or shaly zones that used to be bypassed in the past. Table **2** shows the formation tops and bottoms for the selected four wells.

2.6. Cut-Off Values

There is still no standard procedure for applying physical cut-offs, although they have been utilized for over half a century [25]. However, without standard measurements of cut-offs, there might be significant underestimations of petrophysical algorithms used to evaluate reservoir properties. Cut-offs are required as the reservoir system holds rocks of minimal hydraulic properties non-excludable at the geological correlation stage. The porosity-permeability relationship is the most conventional method utilized to determine porosity cut-off. Moreover, the most commonly used cut-off permeability values for gas and oil are 0.1 and 1.0 mD, respectively. However, these cut-off values are affected by the fluid type of the reservoir and information from core laboratory measurements [30,31]. In this study, the net pay was calculated by utilizing suitable reservoir properties cut-offs in order to exclude uneconomic or unproductive layers. Core porosity versus the logarithm of core permeability was plotted then a semi-log line was fitted through the data points. Porosity cut-off values were established by assuming the same permeability cut-offs for gas and oil as proposed by Bambang [30]. The equivalent porosity was then obtained from the graph corresponding to the selected permeability cut-off that becomes the porosity cut-off. Porosity versus water saturation was plotted based on log analysis data or values from the capillary pressure curves, and the best fit of data was then obtained. The porosity cut-off was then used to obtain the corresponding water saturation (S_W) that becomes the water saturation cut-off. For shaly sands, porosity versus shale volume was plotted. Then porosity cut-off was used, and from the plot, the corresponding shale volume (V_{sh}) can be obtained, which is the cut-off value.

2.7. Estimation of Petrophysical Parameters of Selected Wells

The reservoir zones for the selected wells were identified utilizing the log signatures by eliminating compact and shale beds. Beds with low resistivity, high neutron, high gamma-ray, and low-density readings

Table 2: Ormation Tops for the Four Wells

Well	Formation Top (ft)	Formation Bottom (ft)	Gross Thickness (ft)
A	10087	10153	66
B	10166	10191.5	25.5
C	10142	10216.5	74.5
D	10070	10129.5	59.5

indicated shale. Reservoir zones were identified by porosity, shale volume, and fluid content determinations using the above detailed analysis of well log data and the empirical equations.

3. RESULTS AND DISCUSSION

3.1. Interpretations of Well A Data

The combo-log readings illustrated in Figure **3** were obtained where the GR log gave an estimated clean zone of 15.8 API and shale zone of 191 API. The resistivity of water saturation (R_w) was estimated to be 0.0151 ohm.m. The porosity was estimated from the density log (RHOB) using Equation 4 of the porosity formula with shale correction.

To determine the net-pay thickness of the hydrocarbon-producing zone, the selected porosity cut-off was 12%, while water saturation cut-off was 76% and shale volume cut-off was 9.3% as shown in Figures **4-6**. The obtained net pay thickness was 6.5ft.

Well A was found to have two oil-producing zones based on the cut-off zones that contain non-good characteristics. The interpreted petrophysical properties are summarized in Table **3**.

3.2. Interpretations of Well B Data

The combo-log readings illustrated in Figure **7** were obtained where the GR log gave an estimated clean zone of 45 API and shale zone of 152 API. Rw was

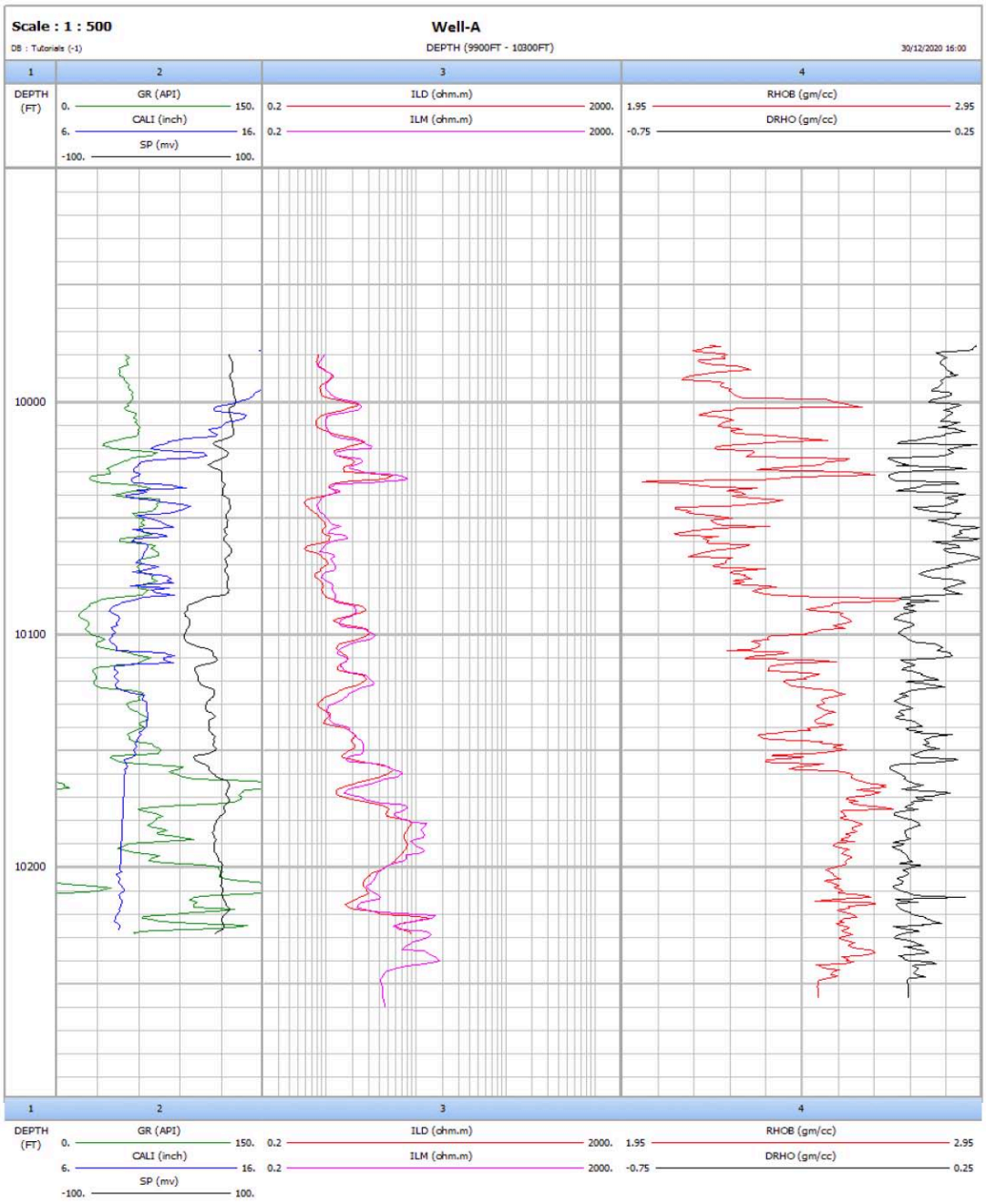

Figure 3: Log data used for determination of depth plot of V_{sh}, S_w and porosity for well A.

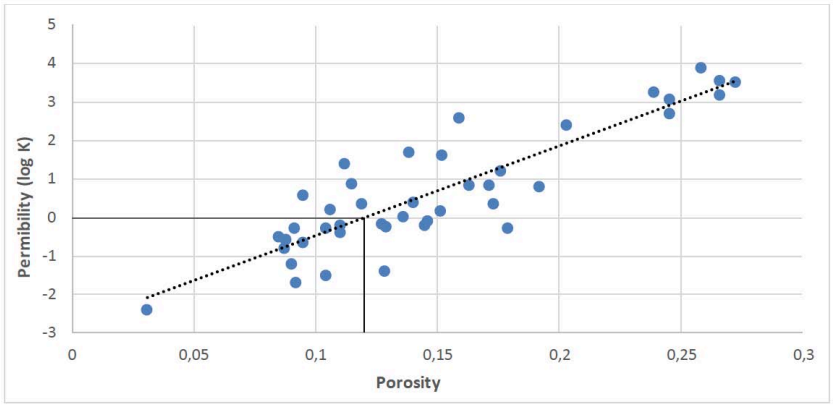

Figure 4: Selection of porosity cut-off for well A.

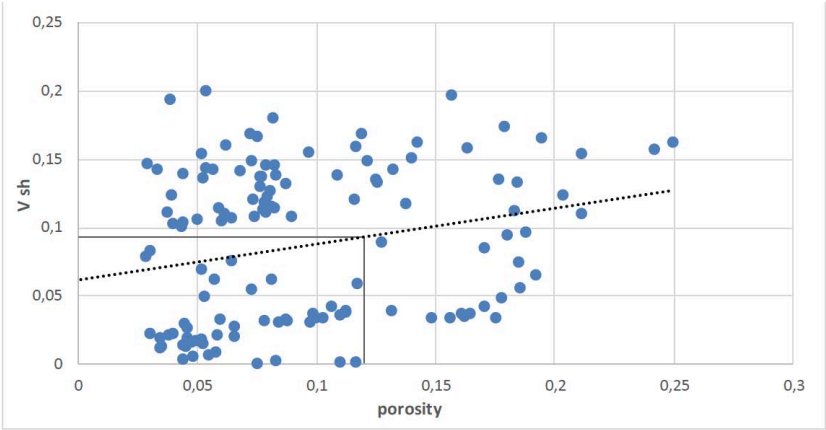

Figure 5: Selection of shale volume cut-off for well A.

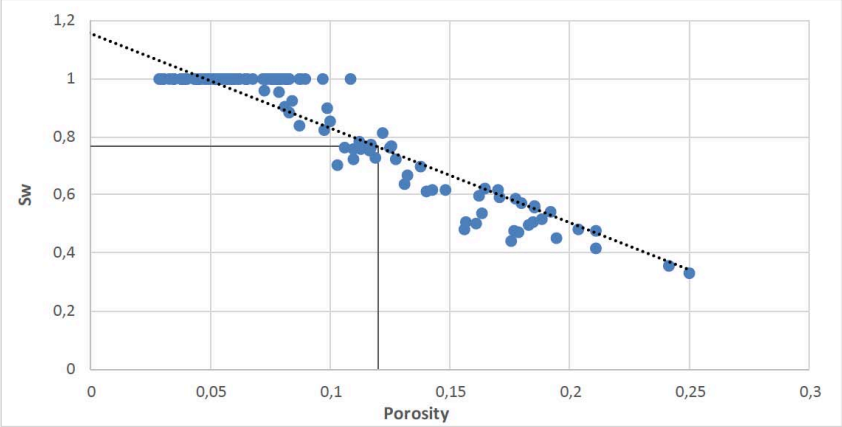

Figure 6: Selection of water saturation cut-off for well A.

Table 3: Summary Results of the Petrophysical Properties of Well A

Zones	Depth (ft)	Net pay thickness (ft)	Ø (%)	Sw (%)	Vsh	K (mD)
1	10104.0 -10108.0	4.5	0.17	0.58	0.1	24.6
2	10117.5-10119.0	2.0	0.15	0.51	0.07	14.1

estimated to be 0.0171 Ohm.m. The porosity was estimated from the sonic log (DT) using Equation 8 of the porosity formula with shale correction.

To determine the net-pay thickness of the hydrocarbon-producing zone, the porosity cut-off was 12%, 62% water saturation cut-off and 9.1% shale

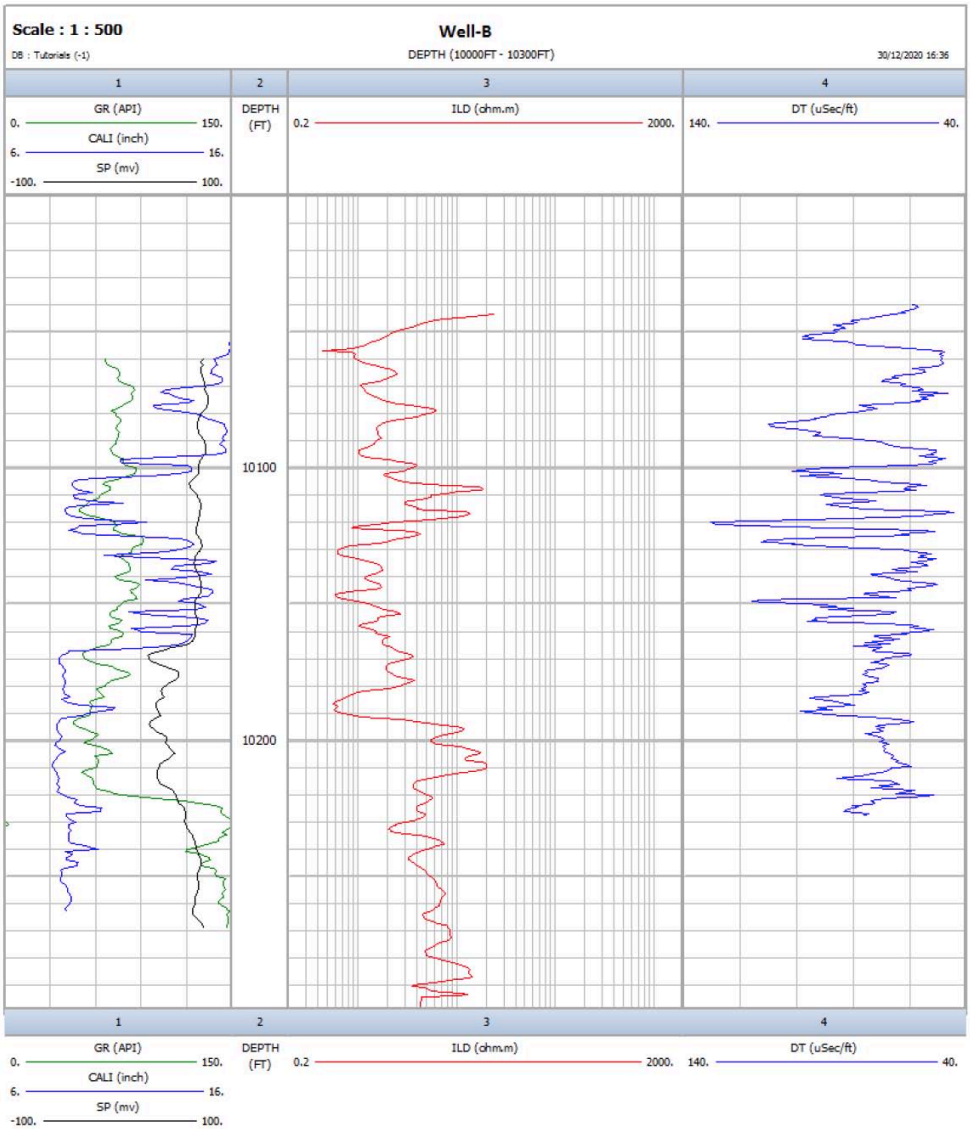

Figure 7: Log data used for determination of depth plot of Vsh, Sw and porosity for well B.

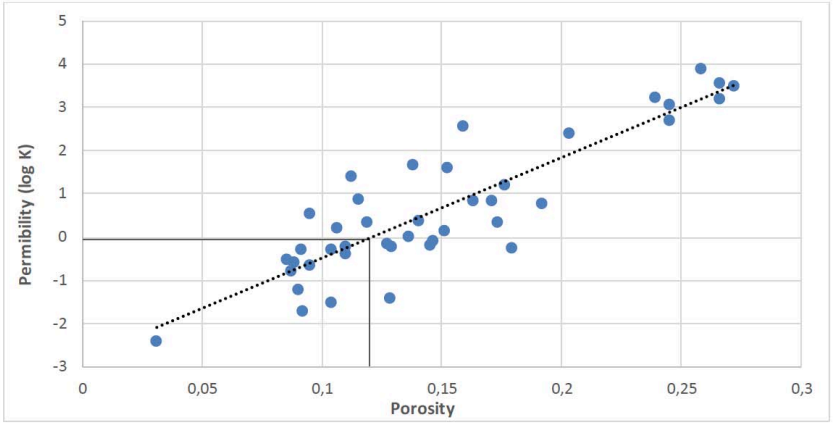

Figure 8: Selection of porosity cut-off for well B.

volume cut-off from Figures **8-10**. Net pay thickness was determined 12.5ft.

Well B was found to have five oil-producing zonation zones based on cut-off zones that contain non-good characteristics. The interpreted petrophysical properties are summarized in Table **4**.

3.3. Interpretations of Well C Data

The combo-log readings illustrated in Figure **11** were obtained as the GR log yielded an estimated clean zone of 16 API and a shale zone of 100 API. Rw was estimated to be 0.0168 Ohm.m. Porosity was

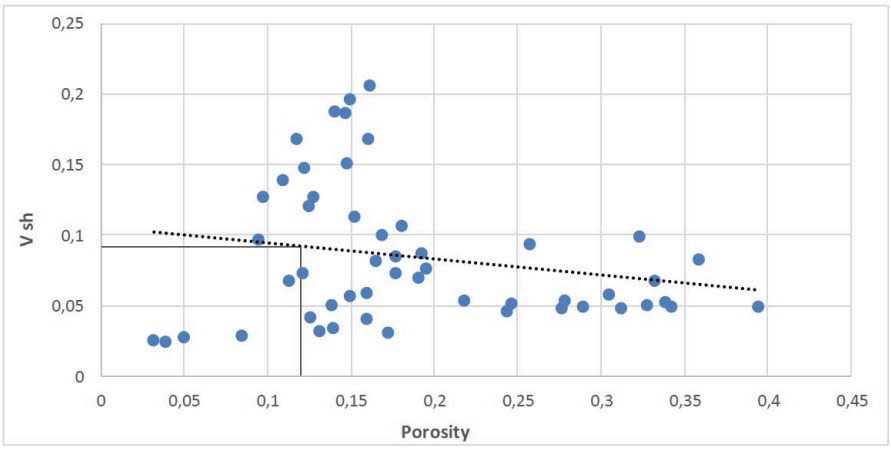

Figure 9: Selection of shale volume cut-off for well B.

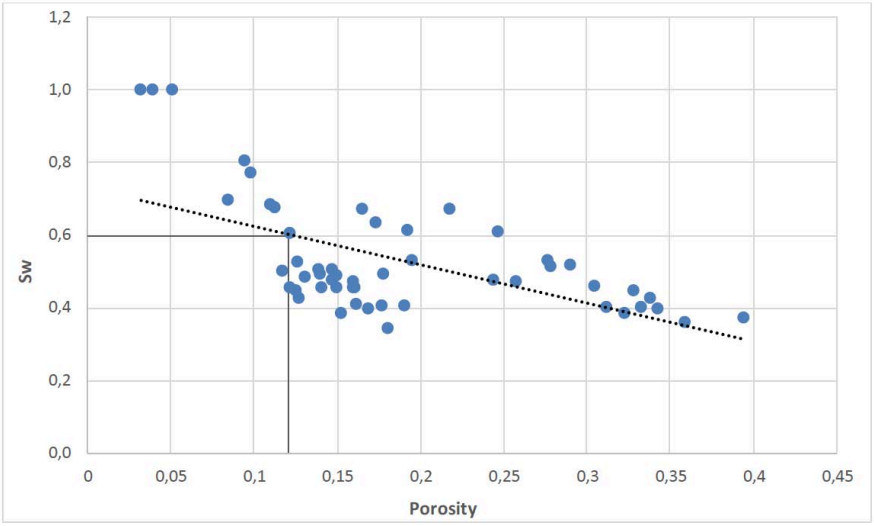

Figure 10: Selection of water saturation cut-off for well B.

Table 4: Summary Results of the Petrophysical Properties of well B.

Zones	Depth (ft)	Net pay thickness (ft)	Ø (%)	Sw (%)	Vsh	K (mD)
1	10166.0-10167.5	2.0	0.14	0.5	0.1	8.0
2	10170.0-10171.5	2.0	0.13	0.49	0.09	4.6
3	10180.5-10182.0	2.0	0.18	0.46	0.15	35
4	10184.5-10186.5	2.5	0.3	0.46	0.12	845
5	10187.5-10191.0	4.0	0.31	0.43	0.1	1096

estimated from a sonic log using Equation 8 of the porosity formula with shale correction.

To determine the net-pay thickness of the hydrocarbon-producing zone, the selected porosity cut-off was 12%, 44% water saturation cut-off, and 12% shale volume cut-off, as shown in Figures **12-14**. Net pay thickness was 12.5ft.

The well has five oil-producing zonation zones based on cut-off zones that contain non-good characteristics. The petrophysical properties are summarized in Table **5**.

3.4. Interpretations of Well D Data

GR, SP, RHOB, NPHI, RT10, N16, DT, Call logs were run in well D and yielded readings at every 0.5ft. The well penetrated the reservoir at a depth of 10101.5-10138.5ft. GR log gave an estimated clean zone of 7 API and a shale zone of 166 API. Rw was estimated at 0.0158 Ohm.m. Porosity was calculated from Equation 4.

To determine the net-pay thickness of the hydrocarbon producing zone, the selected porosity cut-off was12%, 65% water saturation cut-off, and

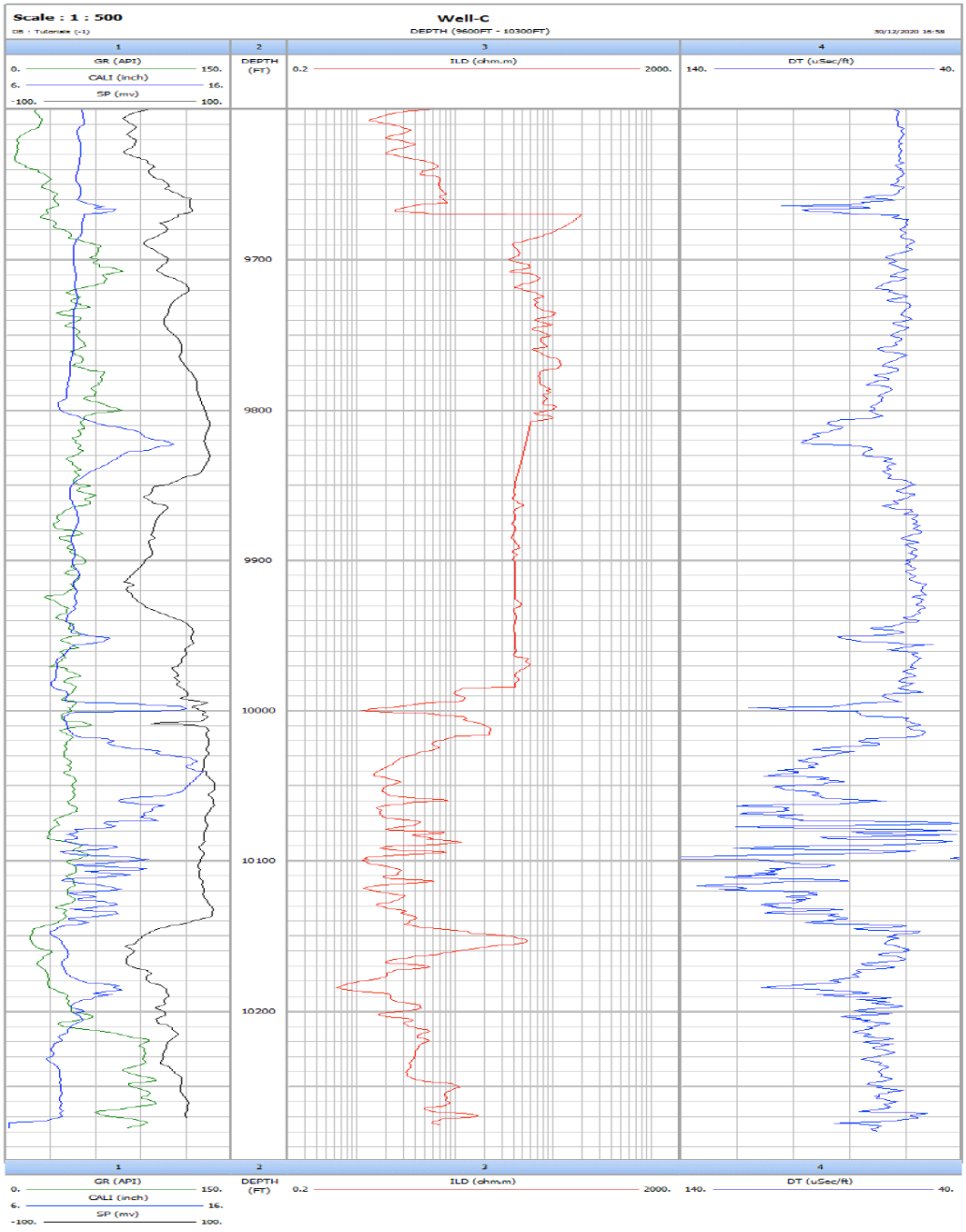

Figure 11: The log data used for determination of depth plot of Vsh, Sw, and porosity for well C.

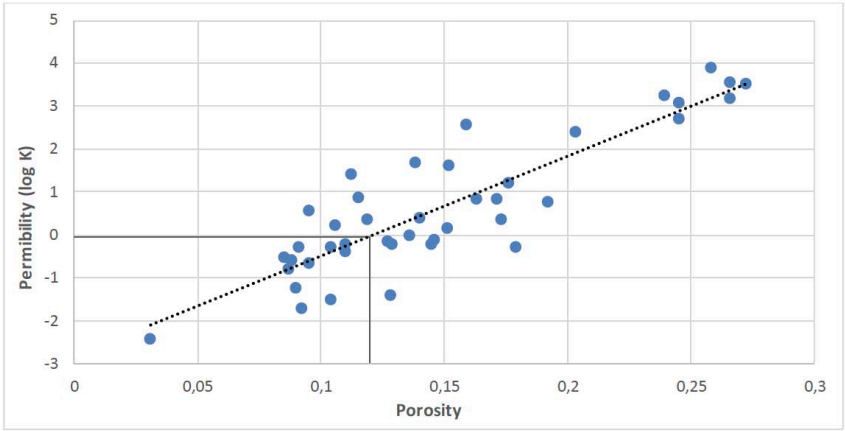

Figure 12: Selection of Porosity cut-off for well C.

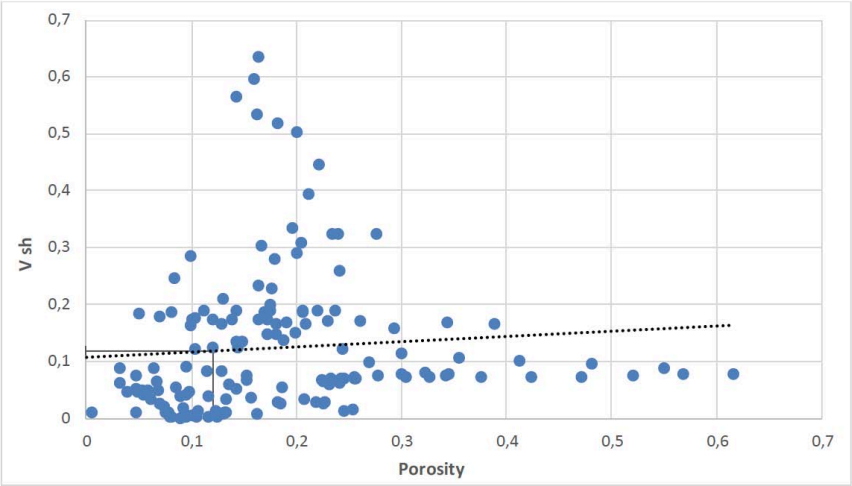

Figure 13: Selection of shale volume cut-off for well C.

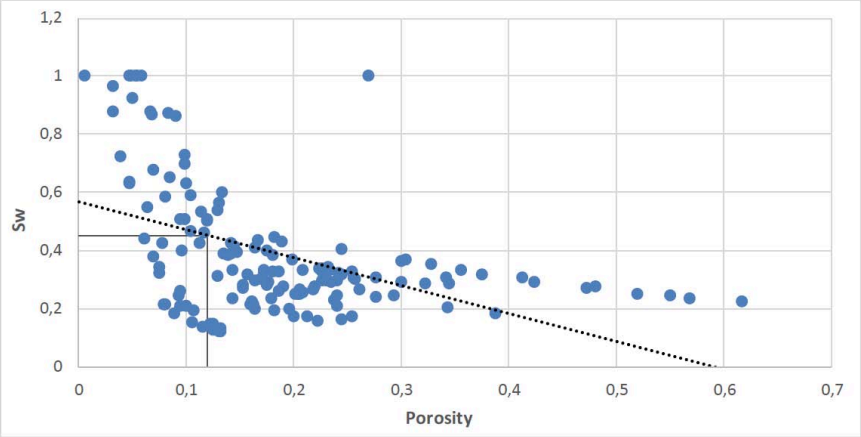

Figure 14: Selection of water saturation cut-off for well C.

Table 5 Summary Results of the Petrophysical Properties of well C.

Zones	Depth (ft)	Net pay thickness (ft)	Ø (%)	Sw(%)	Vsh	K (mD)
1	10144.5-10146.0	2.0	0.21	0.2	0.05	116.5
2	10153.5-10155.5	2.5	0.128	0.13	0.016	3.86
3	10161.5-10163.5	2.0	0.14	0.31	0.11	7.74
4	10168-10170.0	2.5	0.2	0.29	0.059	80.75
5	10171.5-10186.5	15.0	0.26	0.31	0.09	5276

4.9% shale volume cut-off as shown in Figures **16-17**. Net pay thickness was 15.5ft.

The well has five oil-producing zonation zones based on cut-off zones that contain non-good characteristics. The well's petrophysical properties are summarized in Table **6**.

3.5. Cross-Correlation with Core Analysis and other studies

The average computed porosity and permeability for the four wells ranged from 16-26% and 20-3358 mD, respectively. Maximum values of average porosity and permeability are qualitatively very good and good values, respectively. Table **7** shows a summary of the calculated and experimental petrophysical parameters of the wells in the target formation. The calculated findings were in agreement with the experimental data especially the porosity values.

Other findings [32] using well log analysis in southwest Sirte basin reported net pay thickness ranging from 6-153ft, shale between 8-22% volume fraction, a porosity up to 25%, and average water saturation between 35-56%. Thus, the results of the

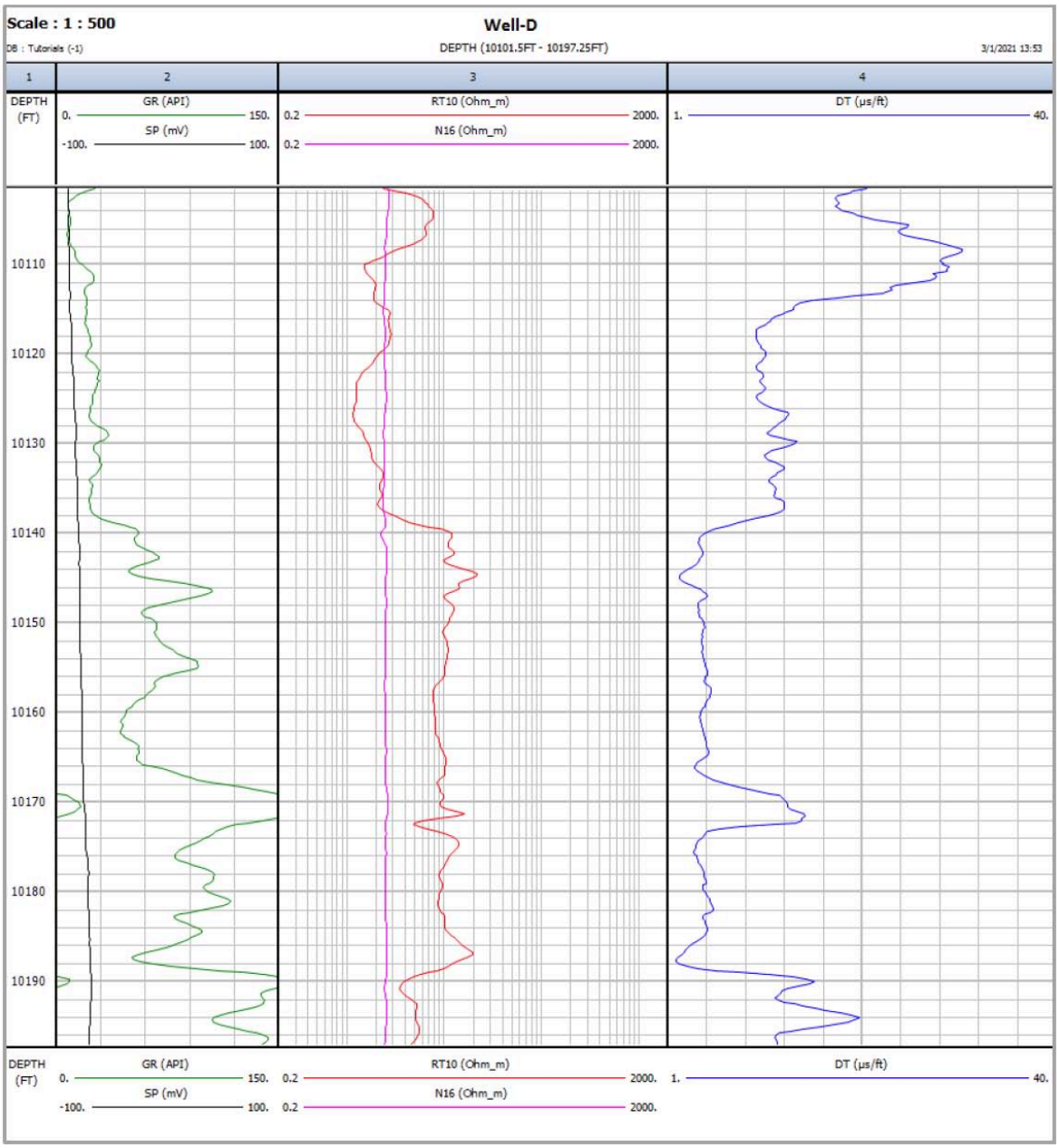

Figure 15: Log data used for determination of depth plot of Vsh, Sw and porosity for well D.

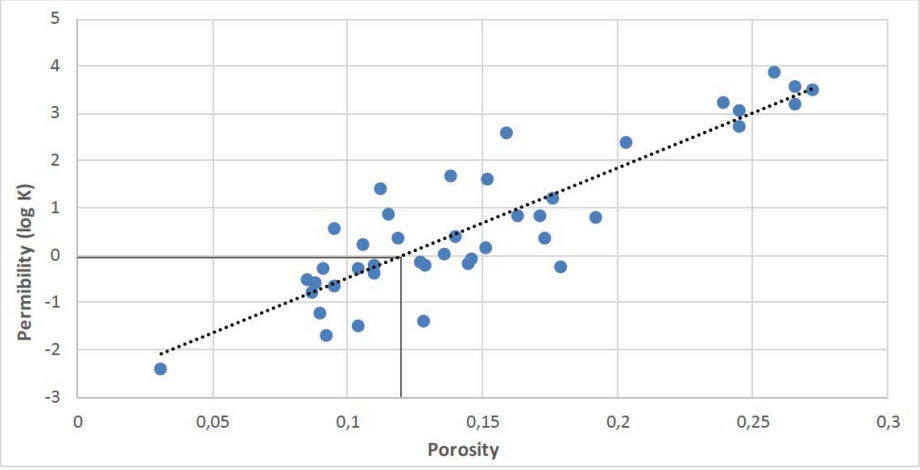

Figure 16: Selection of porosity cut-off for well D.

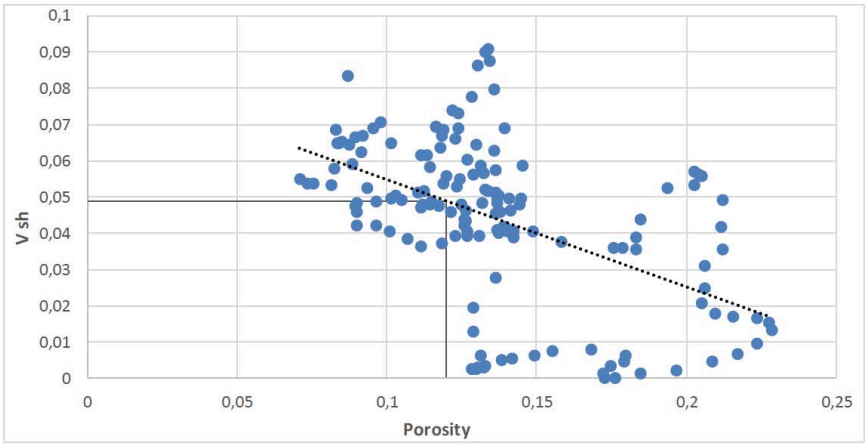

Figure 17: Selection of shale volume cut-off for well D.

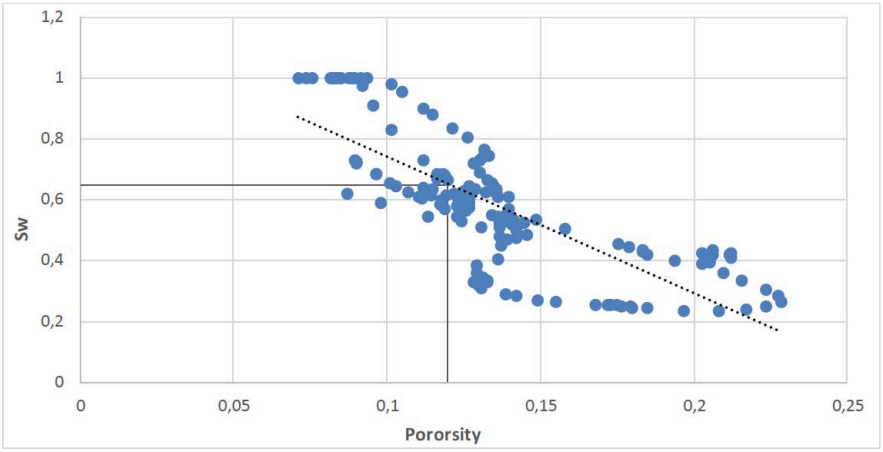

Figure 18: Selection of water saturation cut-off of well D.

Table 6: Summary Results of the Petrophysical Properties of well D.

Zones	Depth (ft)	Net pay thickness (ft)	Ø (%)	Sw(%)	Vsh	K (mD)
1	10101.75-10106.25	4.75	0.14	0.3	0.035	19.3
2	10106.75-10110.5	4.0	0.2	0.31	0.017	139.6
3	10112.25-10116	4.0	0.15	0.48	0.042	25.6
4	10119.5-10120.75	1.5	0.12	0.59	0.041	6.2
5	10135.75-10136.75	1.25	0.13	0.53	0.036	11.4

Table 7: Average Porosity, Permeability, and Formation Water Resistivity for wells in this Study

Well	Ave. Ø (Study)	Ave. Ø (Core)	Average K md (Study)	Average K md (Core)	Rw (ohm-m)
A	16%	15.2%	20	235.7	0.0151
B	23%	16.05%	946	474.6	0.0171
C	26%	NA	3358	NA	0.0168
D	16%	NA	67.6	NA	0.0158

present study are an excellent match with the aforementioned study confirming the general trends of the petrophysical properties within the basin.

4. CONCLUSIONS

A detailed petrophysical analysis of well log data obtained from a mature oil field was performed to

characterize reservoir quality and the remaining hydrocarbon potential with estimation to cut-off values. Results were compared with laboratory measurements and recently published results [32]. The porosity varied from 16 to 26%, and water saturation and permeability ranged from 28 to 57% and 20 to 3300 mD, respectively. The findings were in agreement with the experimental data, and the mature reservoir still contains significant hydrocarbon potential. Formations were found to be mostly continuous intercalated frequently by shale. The method implemented to analyze well logs coupled with cut-off values provided a good insight into the targeted formation petrophysical properties and may be used to analyze and predict other reservoir properties away from the selected wells' locations. Cut-offs on permeability, porosity, water saturation, and shale content greatly affect the economic profitability of a reservoir depletion process. Therefore, they need to be continuously monitored, especially with fast advancing technological techniques and variations in hydrocarbon prices. Moreover, it is important to emphasize that the most important factor in determining cut-off values is permeability.

REFERENCES

[1] Ellis D., Singer J. Well Logging for Earth Scientists (2ed.). Springer Netherlands. 2007. https://doi.org/10.1007/978-1-4020-4602-5

[2] Neog PK, Borah NM. Reservoir characterization through well test analysis assists in reservoir simulation - a case study. SPE Asia Pacific oil and gas conference and exhibition, 2000; 16–18 October, Brisbane, Australia. https://doi.org/10.2118/64447-MS

[3] Joshi GK, Shyammohan V, Reddy AS, Singh B, Chandra M. Reservoir characterization through log property mapping in Geleki field of upper Assam, India. The 5th Conference and exposition on petroleum geophysics, Hyderabad, India. 2004; pp. 685-687.

[4] Ishwar NB, Bhardwaj A. Petrophysical well log analysis for hydrocarbon exploration in parts of Assam-Arakan basin, India. In: 10th Biennial international conference and exposition, society of exploration geophysicists, Kochi, India. 2013; pp. 153.

[5] Ben Mahmud HK, Muhammad Hilmi BMH, Mahmud WM, Van HL, Mian USh Petrophysical interpretations of subsurface stratigraphic correlations, Baram Delta, Sarawak, Malaysia, Energy Geoscience.2020; Volume 1, Issues 3–4, Pages 100-114. https://doi.org/10.1016/j.engeos.2020.04.005

[6] Rider M. The geological interpretation of well log (2ed.). Whittles Publishing, London. 1996; ISBN-13: 978-0954190606.

[7] Mukerji T, Avseth P, Mavko G, Takahashi I, González EF. Statistical rock physics: combining rock physics, information theory, and geo-statistics to reduce uncertainty in seismic reservoir characterization. Lead Edge. 2001; 20(3), pp. 313–319. https://doi.org/10.1190/1.1438938

[8] Sarasty JJ, Stewart RR (2003) Analysis of well-log data from the White Rose oilfield, offshore Newfoundland. CREWES Res Rep 15, pp. 1–16.

[9] Sabila, T., Mahmud, H. K. B., Mahmud, W. M., & Van Dijke, M. I. J.. Two-Phase Oil-Water Empirical Correlation Models for SCAL and Petrophysical Properties in Intermediate Wet Sandstone Reservoirs. IOP Conference Series: Materials Science and Engineering. 2019; 495(1), [012065]. https://doi.org/10.1088/1757-899X/495/1/012065

[10] Mahmud, WM, Ermila, M, Aljahmi, R, Nasr-eddin E. Comparison Between SCAL Measurements and Pore-Scale Network Models for Neutrally Wet Sandstone on Two-Phase Oil-Water Empirical Correlations and Petrophysical Properties." Paper presented at the International Petroleum Technology Conference, Dhahran, Kingdom of Saudi Arabia, January 2020. https://doi.org/10.2523/IPTC-19979-Abstract

[11] Chang HC, Kopaska-Merkel DC, Chen HC. Identification of lithofacies using Kohonen self-organizing maps. Computer Geosciences. 2002; 28, pp. 223-229. https://doi.org/10.1016/S0098-3004(01)00067-X

[12] Khalifa, MK, Jones, BG, Mahmud, WM. Lithostratigraphic and sequence stratigraphic architecture of the Winduck Interval, central Darling Basin, Australia, based on integration of wireline logs, cores and cuttings data. Int J Earth Sci (Geol Rundsch). 2016; 105, 1109–1126 https://doi.org/10.1007/s00531-015-1241-8

[13] Khalifa, MK, Mahmud, WM, Alta'ee, AF *et al*. Sequence stratigraphic analysis of fluvial deposits using facies characterization and wireline log correlation: case of the late Early-early Middle Devonian Snake Cave Interval, Darling Basin, Australia. Arab J Geosci. 2015; 8, 9733–9752. https://doi.org/10.1007/s12517-015-1872-x

[14] Aigbedion JA, Iyayi SE. Formation Evaluation of Oshioka Field, using geophysical well logs Middle-east Journal of Scientific Research 2. 2007; pp. 107-110.

[15] Asquith G, Krygowski D (2004) Relationships of Well Log Interpretation in Basic Well Log Analysis Method in Exploration Series: American Association of Petroleum Geologists, 16, pp. 140. https://doi.org/10.1306/Mth16823C1

[16] SeyedBijan M, Hadi S, Mehdi N, Yaser M. Optimization of reservoir cut-off parameters: a case study in SW Iran. Petroleum Geoscience. 2011; 17, pp. 355-363. https://doi.org/10.1144/1354-079311-005

[17] Thomas SA. The Sirte Basin Province of Libya Sirte-Zelten Total Petroleum System. The US Geological Survey Bulletin. 2001; 2202–F. http://geology.cr.usgs.gov/pub/bulletins/b2202-f/

[18] Anketell JM, Salem MJ, El-Hawat AS, Sbeta AM. Structural history of the Sirt basin and its relationships to the Sabratah basin and Cyrenaican platform, northern Libya. Geology of the Sirte Basin. Elsevier. 1996; 3, pp. 57-88.

[19] Baird DW, Aburawi RM, Bailey NJL. Geohistory and petroleum in the central Sirte Basin. Geology of the Sirte Basin: Elsevier. 1996; 3, pp. 3-56.

[20] Rusk DC. Libya: Petroleum potential of the underexplored basin centers - A twenty-first-century challenge. AAPG Memoir. 2001; 74, pp. 429-452.

[21] Carmalt, SW, Bill St. John. Giant oil and gas fields, in Future Petroleum Provinces of the World: AAPG Memoir. 1986; 40, p. 11-53

[22] Brennan, P. Raguba field-Libya, Sirte Basin, in American Associ ation of Petroleum Geologists Treatise of Petroleum Geology, Atlas of Oil and Gas Fields, Structural Traps VII. 1992; p. 267–289.

[23] Montgomery S. Sirte Basin, North-Central Libya, prospects for the future: Petroleum Frontiers. Petroleum Information Corporation. 1994; 11, pp. 1-94.

[24] MacGregor DS, Moody RTJ. Mesozoic and Cenozoic petroleum systems of North Africa. Petroleum geology of North Africa: Geological Society, Special Publication. 1998; 132, pp. 201–216. https://doi.org/10.1144/GSL.SP.1998.132.01.12

[25] Worthington, PF, Cosentino, L. The Role of Cut-offs in Integrated Reservoir Studies. Paper No: 84387 presented at SPE Annual Technical Conference and Exhibition, Denver, 2003; 5-8 October. https://doi.org/10.2118/84387-MS

[26] Dressor A. Well Logging and Interpretation Techniques: The Course for Home Study Orklahoma (Second Edition). 2004; pp. 692. Springer

[27] Allaud LA, Martin MH. Schlumberger: The history of well log technique. John Wiley & Sons, Inc., New York City. 1977; pp. 333.

[28] Simandoux, P. Dielectric measurements in porous media and application to shaly formation: Revue de L'Institut Français du Pétrole. 1963; v. 18, Supplementary Issue, p. 193–215.

[29] Schlumberger. A guide to wellsite interpretation of the Gulf Coast, Houston, Schlumberger Well Services, Inc. 1975.

[30] Bambang W. An improvised method for determining reservoir rock porosity cut-off with support of laboratory mercury injection data. Paper 143273 presented at SPE Asia Pacific Oil and Gas Conference and Exhibition. 2001; 20-22 September, Jakarta, Indonesia

[31] Mahmud, WM. Effect of Network Topology on Relative Permeability; Network Model and Experimental Approaches. International Journal of Oil, Gas and Coal Engineering. 2017; Vol. 5, No. 5, pp. 90-96. https://doi.org/10.11648/j.ogce.20170505.14

[32] Aldukalia i, BenAbdulhafid Z, Marghani MM. Petrophysical Evaluation of the upper Beda member using Well Logging Analysis in (Balat Field, NC-59, southwest Sirt Basin, Libya). International Science and Technology Journal. 2020; Volume 23. pp 2-18.

Received on 25-11-2020 Accepted on 29-12-2020 Published on 31-12-2020

DOI: https://doi.org/10.15377/2409-787X.2020.07.5